IJISET - International Journal of Innovative Science, Engineering & Technology, Vol. 3 Issue 11, November 2016
ISSN (Online) 2348 – 7968 | Impact Factor (2015) - 4.332
www.ijiset.com

Analysis of Single Point Incremental Forming Process to Fabricate Phosphorous Bronze Hemispherical Cups

G. Soujanya[1] and A. Chennakesava Reddy[2]

[1] P G Student, Department of Mechanical Engineering, JNT University Hyderabad, Hyderabad, Telangana, India

[2] Professor, Department of Mechanical Engineering, JNT University Hyderabad, Hyderabad, Telangana, India

Abstract

The purpose of this work was to determine the formability of phosphorous bronze alloy to fabricate hemispherical cups using single point incremental forming (SPIF) process. The finite element analysis has been carried out to model the single point incremental forming process using ABAQUS software code. The process parameters of SPIF were sheet thickness, step depth, tool radius and coefficient of friction. The process parameters have been optimized using Taguchi techniques. The major process parameters influencing the SPIF of hemispherical cups were sheet thickness, step size and coefficient of friction.

Keywords: *phosphorous bronze, hemispherical cup, single point incremental forming, finite element analysis, step depth, tool radius, sheet thickness, coefficient of friction.*

1. Introduction

Deep drawing is a process for shaping sheets into cup-shaped articles without excessive localized thinning. The properties of metals and alloys such as materials, such as AA1050 alloy [1], AA2014 alloy [2], AA3003 alloy [3], AA5052 alloy [4], Ti-Al-4V alloy [5], EDD steel [6], are greatly influenced by their microstructure, which may be revised by alloying elements, by heating or heat treatment or by plastic deformation. Progress in sheet metal forming technology is also associated with development of new techniques for sheet metal cutting.

Single point incremental forming (SPIF) is a new sheet metal forming process in which forming takes place by local stretching of the sheet with a round nose tool following a tool path controlled by a CNC machine [7, 8]. The main process variables in SPIF are sheet thickness, coefficient of friction, tool radius, drawing angle, downward step depth per revolution [9-14]. This process can be employed to form complex shapes using CNC milling machine.

The present work was to study the formability of hemispherical cups of phosphorous bronze using SPIF. For this purpose, the design of experiments was executed as per Taguchi technique. The process parameters of SPIF were sheet thickness, step depth, tool radius and coefficient of friction. The formability was evaluated using finite element method.

2. Materials and Methods

In the present work, ABAQUS (6.14) software code was used for the numerical simulation of SPIF process to fabricate hemispherical cups. The material was phosphorous bronze. The SPIF process parameters were chosen at three levels as summarized in table 1. The orthogonal array (OA), L9 was preferred to carry out experimental and finite element analysis (FEA) as given in table 2.

Table 1: Process parameters and levels

Factor	Symbol	Level–1	Level–2	Level–3
Sheet thickness, mm	A	0.8	1.0	1.2
Step depth, mm	B	0.50	0.75	1.00
Tool radius, mm	C	4.0	5.0	6.0
Coefficient of friction	D	0.15	0.175	0.20

The sheet and tool geometry were modeled as deformable and analytical rigid bodies, respectively, using ABAQUS. They were assembled as frictional contact bodies. The sheet material was meshed with S4R shell elements (figure 2a). The fixed boundary conditions were given to all four edges of the sheet. As shown in figure 2b. The boundary conditions for tool were x, y, z linear movements and rotation about the axis of tool. True stress-true strain experimental data were loaded in the tabular form as material properties. The tool path geometry was generated using CAM software [15] was imported to the ABAQUS as shown in figure 3. The elastic-plastic deformation analysis was carried out for the equivalent stress, strain and strain rates and thickness variation.

Table 2: Orthogonal Array (L9) and control parameters

Treat No.	A	B	C	D
1	1	1	1	1
2	1	2	2	2
3	1	3	3	3
4	2	1	2	3
5	2	2	3	1
6	2	3	1	2
7	3	1	3	2
8	3	2	1	3
9	3	3	2	1

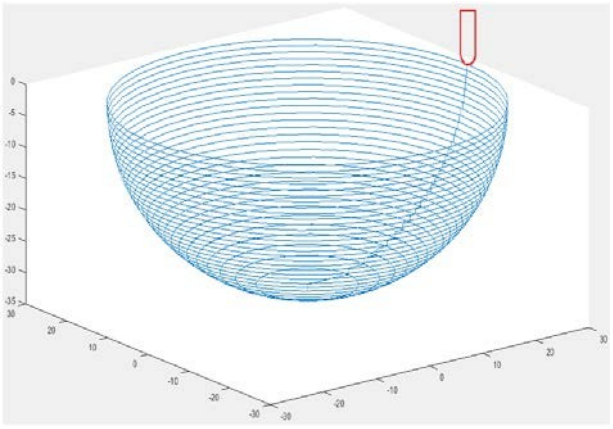

Fig.1 Tool path generation.

3. Results and Discussion

The influence of process variables on the von Mises stress, strain rate and thickness reduction are discussed. The formability limit diagrams are also constructed.

Table 3: ANOVA summary of the von Mises stress.

Source	Sum 1	Sum 2	Sum 3	SS	v	V	P
A	1151.44	1170.30	1246.55	1690.73	2	845.37	62.86
B	1176.74	1184.37	1207.18	167.30	2	83.65	6.22
C	1220.47	1171.78	1176.05	484.65	2	242.32	18.02
D	1215.68	1178.27	1174.35	346.98	2	173.49	12.90
e				0.00	0		0.00
T	4764.31	4704.72	4804.13	2689.66	8		100.00

Note: *SS is the sum of square, v is the degrees of freedom, V is the variance, P is the percentage of contribution and T is the sum squares due to total variation.*

Influence of process parameters on effective stress

Table – 3 gives the ANOVA (analysis of variation) summary of von Mises stress data. The percent contribution specifies that sheet thickness, A, contributes 62.86%, step depth, B, accords 6.22%, tool radius, C, presents 18.02% and coefficient of friction, D, bequests 12.90% of total variation on the von Mises stress.

Fig. 2 presents the influence of SPIF process variables on von Mises stress induced in phosphorous bronze. The von Mises stress increases with increasing sheet thickness (Fig. 2a). This can be endorsed that the force required for the plastic deformation increases with increasing sheet thickness. Fig. 2a describes the von Mises stress as a function of step depth. The von Mises stress increases with increasing step depth. The von Mises stress decreases with increasing of tool radius and coefficient of friction as shown in Fig. 2b. As observed from Figs. 3 to 5, that the von Mises stress increases with increasing strain up to 0.5 and later on it slightly decreases. The energy dissipated in the plane strain region is less than that dissipated in the shear lips. This is due to the higher stress triaxiality in this zone that favors the micro-mechanisms of damage. These occur for a low strain, which corresponds a low density of plastic deformation energy.

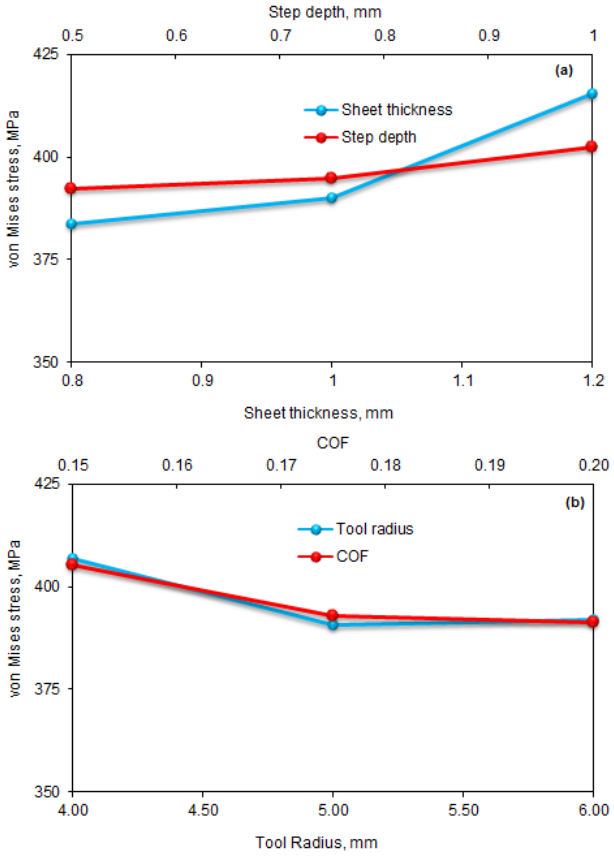

Fig. 2 Influence of process variables on von Mises stress.

ISSN (Online) 2348 – 7968 | Impact Factor (2015) - 4.332
www.ijiset.com

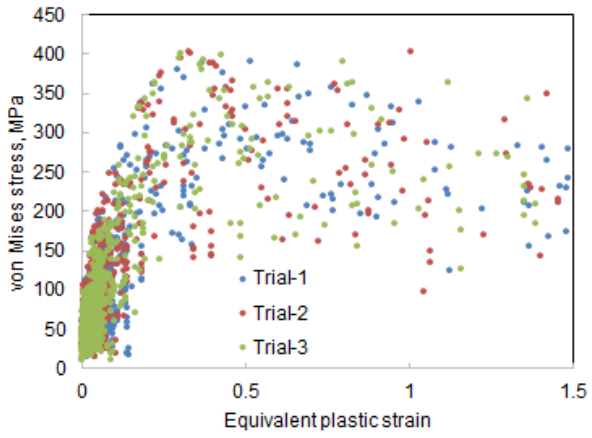

Fig. 3 Equivalent plastic strain vs equivalent stress for trials 1, 2 and 3.

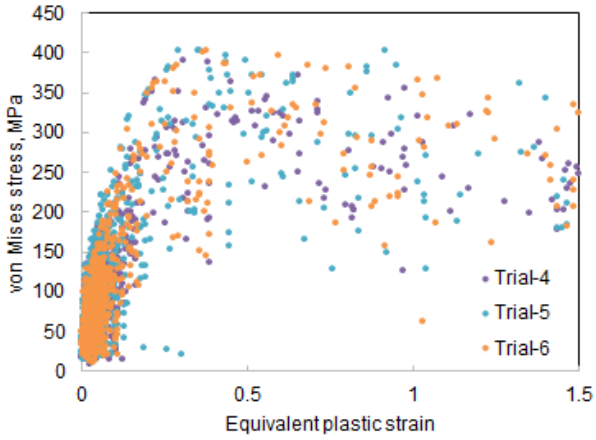

Fig. 4 Equivalent plastic strain vs equivalent stress for trials 4, 5 and 6.

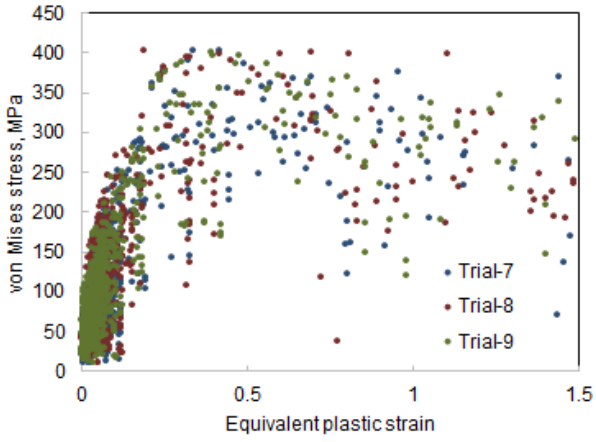

Fig. 5 Equivalent plastic strain vs equivalent stress for trials 7, 8 and 9.

For the trials 1, 2 and 3, the von Mises stresses are, respectively, 403.4, 402.9 MPa and 402.5 MPa as shown in Fig.6. For the trials 4, 5 and 6, the von Mises stresses are, respectively, 398.4, 403.4 and 403.3 MPa as shown in Fig.7. For the trials 7, 8 and 9, the von Mises stresses are, respectively, 403.3, 401.4 and 403.4 MPa as shown in Fig. 9. The ultimate tensile strength of phosphorous bronze is 480 MPa, which is not exceeded in all the trials.

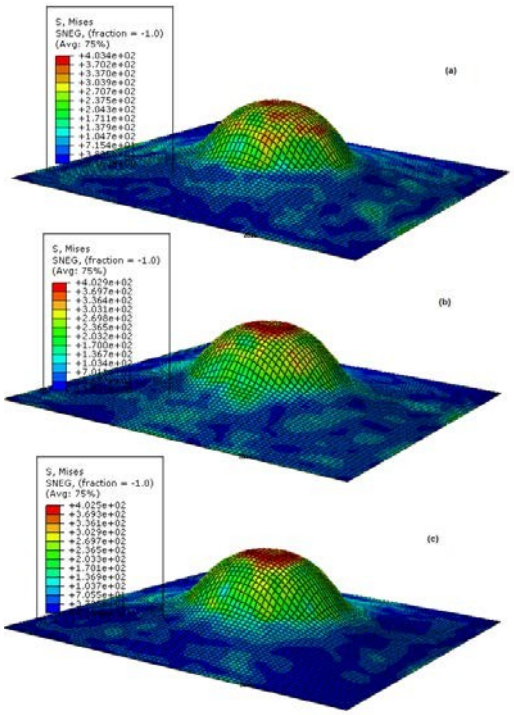

Fig. 6 Raster images of von Mises stress in the cups for trials 1, 2 and 3.

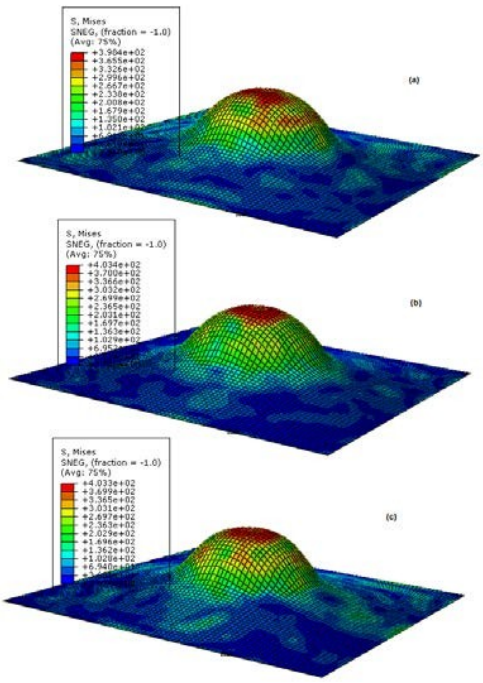

Fig. 7 Raster images of von Mises stress in the cups for trials 4, 5 and 6.

ISSN (Online) 2348 – 7968 | Impact Factor (2015) - 4.332
www.ijiset.com

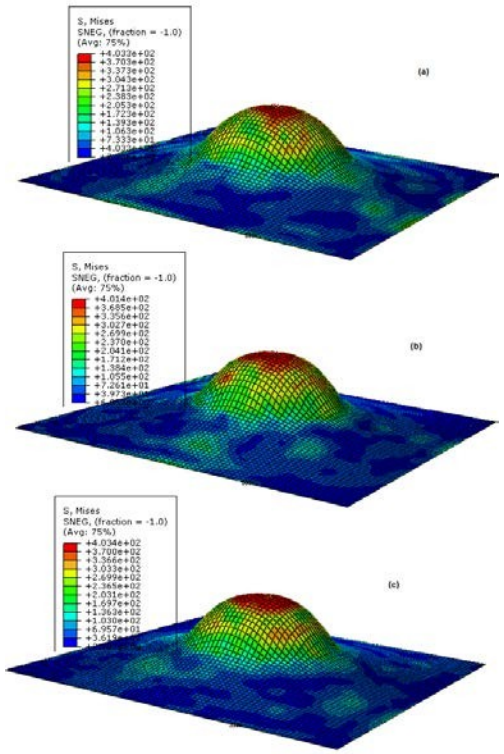

Fig. 8 Raster images of von Mises stress in the cups for trials 7, 8 and 9.

3.2 Influence of parameters on strain rate

The ANOVA summary of the strain rate is given in Table **4.** The percent contribution column establishes the major contributions 69.54%, 22.24%, 4.45% and 3.77% of step depth, tool radius, coefficient of friction, sheet thickness, respectively, towards variation in the strain rate.

Table 4: ANOVA summary of the strain rate

Source	Sum 1	Sum 2	Sum 3	SS	v	V	P
A	0.9204	0.7674	0.8368	0.00391	2	0.00196	3.77
B	1.1236	0.9206	0.4803	0.07210	2	0.03605	69.54
C	0.6278	0.9667	0.9301	0.02306	2	0.01153	22.24
D	0.89	0.8925	0.7455	0.00461	2	0.00231	4.45
E				1.11E-16	0		0
T	3.56	3.55	2.99	0.10	8		100.00

The strain rate decreases with increase of sheet thickness from 0.8 to 1.0 mm and later on it increases a little for the sheet thickness of 1.2 mm as shown in Fig. 9a. The strain rate decreases with increase of step depth as shown in Fig.9a. For smaller step size, local deformation plays an important role than stretching. As observed from Fig. 9b, the strain rate is found to be high for tool radius of 5 mm. during the plastic deformation of sheet material. The frictional shear stress is directly proportional to the coefficient of friction as per Coulomb's law of friction ($\tau = \mu F_n$, where F_n is the normal pressure). When the frictional shear stress, reaches the limiting shear stress of the sheet material, the material undergoes plastic deformation. For higher value of COF (coefficient of friction) smaller value of von Mises stress implies that the blank has stretched (Fig. 9b).

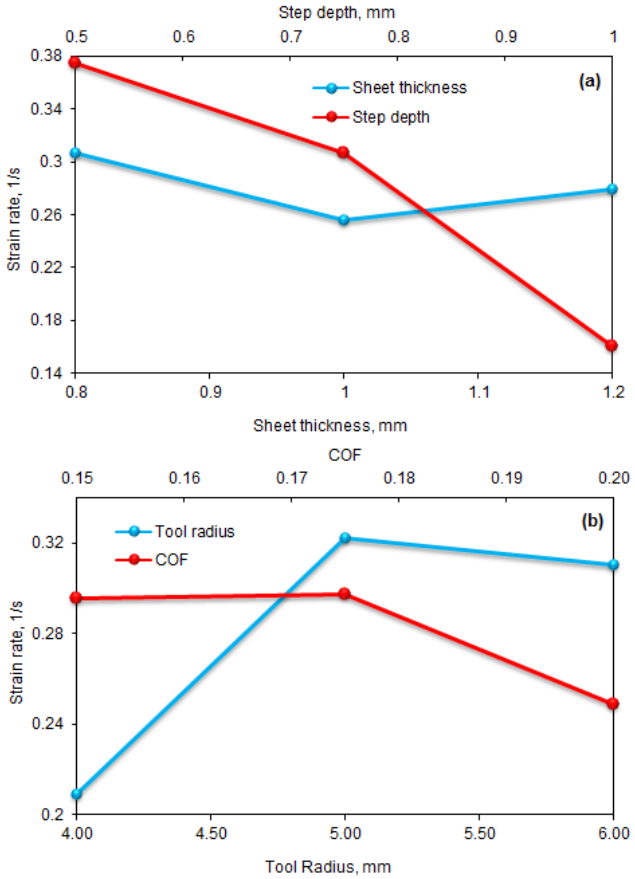

Fig. 9 Influence of process variables on strain rate.

3.3 Influence of parameters on thickness reduction

The ANOVA summary of the thickness reduction is given in Table 5. The only one process variable that influences variation in the thickness reduction is the sheet thickness and the rest of the variables are least considered.

Table 5: ANOVA summary of the thickness reduction

Source	Sum 1	Sum 2	Sum 3	SS	v	V	P
A	1.19	1.54	1.90	0.08	2.00	0.04	99.47
B	1.55	1.54	1.54	0.00	2.00	0.00	0.05
C	1.56	1.55	1.52	0.00	2.00	0.00	0.44
D	1.55	1.54	1.55	0.00	2.00	0.00	0.04
e				0.00	0.00		0.00
T	5.86	6.16	6.51	0.08	8.00		100.00

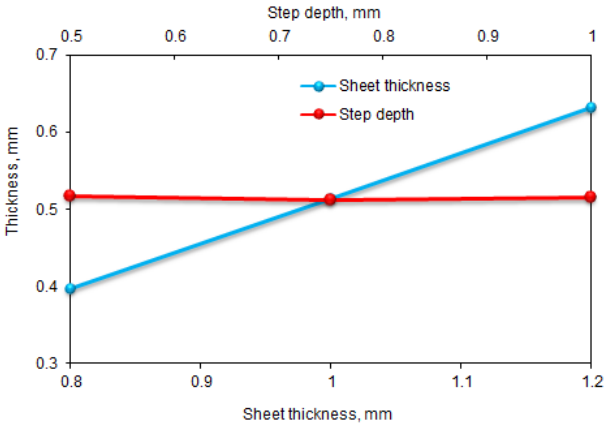

Fig. 10 Influence of process parameters on thickness reduction.

The reduction of sheet thickness increases with increasing sheet thickness as shown in Fig.10. The reduction of thickness is considered at the centerline of the deformed cup as shown in Fig. 11. As observed from Fig.11, the majority of thickness reduction takes place in the walls of the cup but not in the flange or bottom of the cup. The elements located at the mid regions of the walls are elongated higher than those present at the top and bottom of the cup walls.

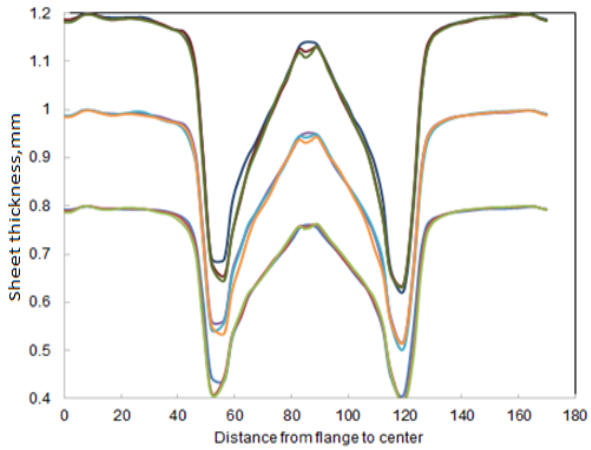

Fig. 11 Location of thickness reduction in the deformed cup.

3.4 Formability of SPIF process

The formability diagrams of the cups are shown in Figs.12 to 14. During initial stages of SPIF, the shear and compressive stresses are dominating the formability of hemispherical cups. Over the strain values of 0.3, the tension is highly predominant resulting the stretching sheet. As the sheet thickness decreases, the formability curve moves towards uni-axial tension line. Effect of bi-axial tension is not observed in the SPIF process.

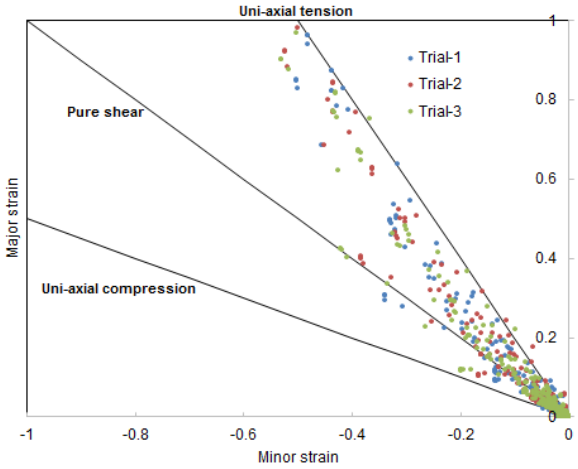

Fig. 12 Formability limit diagrams for trials 1, 2 and 3.

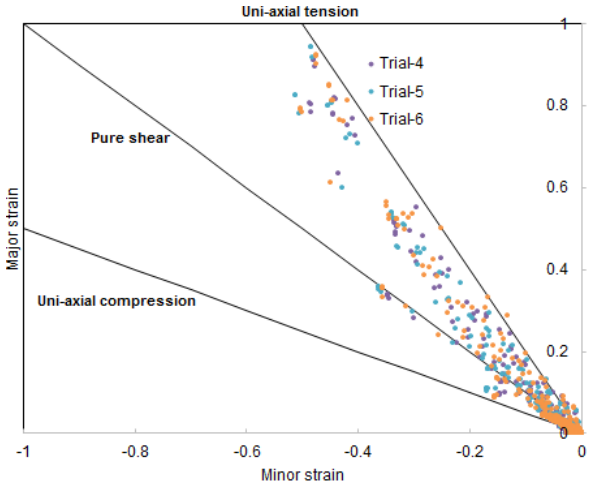

Fig. 13 Formability limit diagrams for trials 3, 4 and 5.

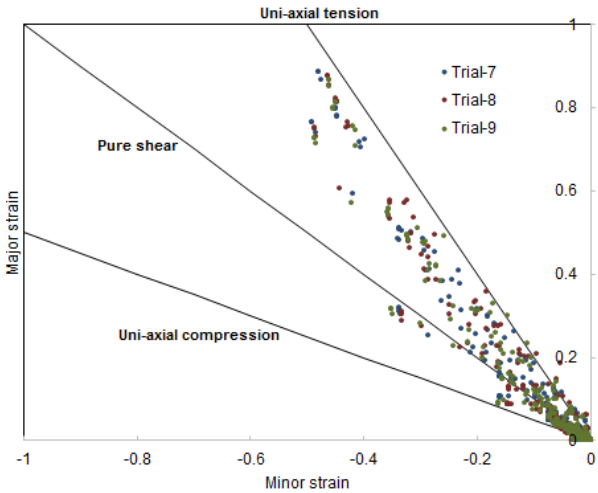

Fig. 14 Formability limit diagrams for trials 7,8 and 9.

ISSN (Online) 2348 – 7968 | Impact Factor (2015) - 4.332

www.ijiset.com

4. Conclusions

The foremost SPIF process variables, which influence the von Mises stress, strain rate and thickness reduction of hemispherical cups of phosphorous bronze alloy, were sheet thickness, step size and coefficient of friction. The formability limit diagram was highly influenced by the sheet thickness.

Acknowledgments

The author acknowledges with thanks University Grants Commission (UGC) – New Delhi for sectioning R&D project.

References

[1] A. C. Reddy, "Homogenization and Parametric Consequence of Warm Deep Drawing Process for 1050A Aluminum Alloy: Validation through FEA," International Journal of Science and Research, vol. 4, no.4, pp. 2034-2042, 2015.

[2] A. C. Reddy, "Parametric Optimization of Warm Deep Drawing Process of 2014T6 Aluminum Alloy Using FEA," International Journal of Scientific & Engineering Research, vol. 6, no. 5, pp.1016-1024, 2015.

[3] A. C. Reddy, "Practicability of High Temperature and High Strain Rate Superplastic Deep Drawing Process for AA3003 Alloy Cylindrical Cups," International Journal of Engineering Inventions, vol. 5, no. 3, pp. 16-23, 2016.

[4] A. C. Reddy, "Suitability of High Temperature and High Strain Rate Superplastic Deep Drawing Process for AA5052 Alloy," International Journal of Engineering and Advanced Research Technology, vol. 2, no.3, pp. 11-14, 2016.

[5] A.C. Reddy, "Finite element analysis of reverse superplastic blow forming of Ti-Al-4V alloy for optimized control of thickness variation using ABAQUS," Journal of Manufacturing Engineering, vol. 1, no.1, pp.6-9, 2006.

[6] A. C. Reddy, T. K. K. Reddy, M. Vidya Sagar, "Experimental characterization of warm deep drawing process for EDD steel," International Journal of Multidisciplinary Research & Advances in Engineering, vol. 4, no.3, pp.53-62, 2012.

[7] E. Leszak, "Apparatus and process for incremental dieless forming," Patent US3342051A, 1967.

[8] K. Kitazawa, A. Wakabayashi, K. Murata, K. Yaejima, "Metal-flow phenomena in computerized numerically controlled incremental stretch-expanding of aluminum sheets," Keikinzoku Journal of Japan Institute of Light Metals, vol. 46, pp. 65-70, 1996.

[9] V. Srija, A. C. Reddy, "Numerical Simulation of Truncated Pyramidal Cups of AA1050-H18 Alloy Fabricated by Single Point Incremental Forming," International Journal of Engineering Sciences & Research Technology, vol. 5, no. 6, pp. 741-749, 2016.

[10] T. Santhosh Kumar, A. C. Reddy, "Single Point Incremental Forming and Significance of its Process Parameters on Formability of Conical Cups Fabricated From AA1100-H18 Alloy, International Journal of Engineering Inventions," vol. 5, no. 6, pp. 10-18, 2016.

[11] A. Raviteja, A. C. Reddy, "Implication of Process Parameters of Single Point Incremental Forming for Conical Frustum Cups From AA 1070 using FEA," International Journal of Research in Engineering and Technology, vol. 5, no.6, pp. 124-129, 2016.

[12] T. Santhosh Kumar, V. Srija, A. Ravi Teja, A. C. Reddy, "Influence of Process Parameters of Single Point incremental Deep Drawing Process for Truncated Pyramidal Cups from 304 Stainless Steel using FEA," International Journal of Scientific & Engineering Research, vol. 7, no. 6, pp. 100-105, 2016.

[13] C. R. Alavala, "FEM Analysis of Single Point Incremental Forming Process and Validation with Grid-Based Experimental Deformation Analysis," International Journal of Mechanical Engineering, vol. 5, no. 5, pp. 1-6, 2016.

[14] C. R. Alavala, "Validation of Single Point Incremental Forming Process for Deep Drawn Pyramidal Cups using Experimental Grid-Based Deformation," International Journal of Engineering Sciences & Research Technology, vol. 5, no. 8, pp. 481-488, 2016.

[15] C. R. Alavala, "CAD/CAM: Concepts and Applications," New Delhi: PHI Learning Pvt. Ltd, 2008.